BIOCHEMICAL PHARMACOLOGY 73 (2007) 1910–1926

available at www.sciencedirect.com

journal homepage: www.elsevier.com/locate/biochempharm

Activity of piperaquine and other 4-aminoquinoline antiplasmodial drugs against chloroquine-sensitive and resistant blood-stages of *Plasmodium falciparum* Role of β-haematin inhibition and drug concentration in vacuolar water- and lipid-phases

David C. Warhurst [a,*], *John C. Craig* [b], *Ipemida S. Adagu* [a], *R. Kiplin Guy* [b,1], *Peter B. Madrid* [b,2], *Quinton L. Fivelman* [a]

[a] *Pathogen Molecular Biology Unit, Department of Infectious and Tropical Diseases, London School of Hygiene and Tropical Medicine, University of London, Keppel Street, London WC1E 7HT, UK*
[b] *Department of Pharmaceutical Chemistry, University of California, San Francisco, CA 94143-0446, USA*

ARTICLE INFO

Article history:
Received 11 January 2007
Accepted 12 March 2007

Keywords:
Plasmodium
4-Aminoquinolines
Piperaquine
Lysosomotropism
Drug-resistance
Hydrophobicity

ABSTRACT

Chloroquine (CQ), a 4-aminoquinoline, accumulates in acidic digestive vacuoles of the malaria parasite, preventing conversion of toxic haematin to β-haematin. We examine how *bis* 4-aminoquinoline piperaquine (PQ) and its hydroxy-modification (OH-PQ) retain potency on chloroquine-resistant (CQ-R) *Plasmodium falciparum*. For CQ, PQ, OH-PQ and **4** and **5**, representing halves of PQ, β-haematin inhibitory activity (BHIA) was assayed, while potency was determined in CQ-sensitive (CQ-S) and CQ-R *P. falciparum*. From measured pK_as and the pH-modulated distribution of base between water and lipid (log D), the vacuolar accumulation ratio (VAR) of charged drug from plasma water (pH 7.4) into vacuolar water (pH 4.8) and lipid accumulation ratio (LAR) were calculated. All agents were active in BHIA. In CQ-S, PQ, OH-PQ and CQ were equally potent while **4** and **5** were 100 times less potent. CQ with two basic centres has a VAR of 143,482, while **4** and **5**, with two basic centres of lower pK_as have VARs of 1287 and 1966. In contrast PQ and OH-PQ have four basic centres and achieve VARs of 104,378 and 19,874. This confirms the importance of VAR for potency against CQ-S parasites. Contrasting results were seen in CQ-R. **5**, PQ and OH-PQ with LARs of 693; 973,492 and 398,118 (compared with 8.25 for CQ) showed similar potency in CQ-S and CQ-R. Importance of LAR for potency against CQ-R parasites probably reflects ability to block efflux by hydrophobic interaction with PfCRT but may relate to β-haematin inhibition in vacuolar lipid.

* *Corresponding author*. Tel.: +44 207 927 2341; fax: +44 207 637 0248.
E-mail address: david.warhurst@lshtm.ac.uk (D.C. Warhurst).
[1] Present address: Biosciences Division, SRI International, 333, Ravenswood Avenue, Menlo Park, CA 94025, USA.
[2] Present address: Department of Chemical Biology and Therapeutics, St. Jude Children's Research Hospital, 332 North Lauderdale, Memphis, TN 38105, USA.
0006-2952/$ – see front matter
doi:10.1016/j.bcp.2007.03.011

1. Introduction

With the increasing spread of drug-resistance to the 4-amino-7-chloroquinoline base chloroquine (CQ) (**1**) (Fig. 1) in the malaria parasite *Plasmodium falciparum* [1] and the associated raised case-mortality in children [2], a number of related *bis* 4-amino quinolines have been investigated. These compounds contain two 4-amino-7-chloroquinoline moieties connected at the 4-amino group by a variable linker group [3].

One such group, the *bis*-quinolin-4-yl piperazines, yielded several active antimalarials. In particular, the (7-chloroquinolin-4-yl)-*N*-1′ piperazine) dimers piperaquine (PQ) **2** originally reported by Rhone-Poulenc as 13,228 RP and hydroxypiperaquine (OH-PQ) **3** (Fig. 1), in which the *N*-1′ atom of a piperazine linker was directly attached to the C-4 position of each quinoline. PQ and OH-PQ were active ip against *P. berghei* in mice [4]. PQ was orally effective against blood-induced *P. cynomolgi* in rhesus monkeys and was then proved in *P. falciparum* infections in man [5]. There was evidence of persistence of active drug levels in the mouse for 15–30 days after a single ip dose [6,7].

Later, following the extension of the CQ-resistance problem, both PQ and OH-PQ were resynthesized in China [8], and successfully applied by Prof. Chen Lin and colleagues, to the treatment and prevention of infections with CQ-resistant *P. falciparum* on Hainan Island [9]. While as potent as CQ in a CQ-sensitive strain, PQ is reported six times more active than CQ in CQ-resistant *P. falciparum in vitro* [10]. More recent studies have confirmed the value of PQ in multidrug resistance [11] and its utility as a companion drug for the endoperoxides dihydroartemisinin and artesunate [12].

There can be no doubt that the release of free haematin from haemoglobin during digestion [13] is the basis of CQ's selective toxicity for intraerythrocytic malaria parasites [14]. The acidic content of the digestive vacuole (lysosome), where the haematin is released, is the site of concentration of this weakly basic 4-amino-7-chloroquinoline drug [15–18], which binds to haematin and prevents its detoxification by cyclic dimerization [19]. Although the concentration of protonated CQ2H+ into vacuolar water appears to be a requirement for antimalarial activity [15,16,20,21], recent studies indicate that haematin dimerization and detoxication may take place in or closely associated with lipid droplets in the interior of the vacuole [22,23]. The rate of development in cell-free systems of the insoluble crystal of malaria pigment, haemozoin or β-haematin [19], is enhanced by presence in the acidic buffer (pH 4.8) of the long chain alcohol *n*-octanol or other neutral lipids [23,22]. The importance of lipid for haemozoin formation highlights alternative possibilities for different drugs, that drug/haematin complexes may form in the vacuolar water and transfer to lipid sites where inhibition of dimerization takes place, or that haematin within the lipid may complex with uncharged drug already localized there. Experimentally it can be demonstrated that [^{3}H] CQ becomes incorporated into β-haematin during its formation in cell-free systems and in intact infected erythrocytes [24], but it is not yet clear what significance this has for the mode of action. In CQ-R *P. falciparum* blood stages, equilibrium concentration of CQ within the infected cell is diminished [25] probably through efflux [26], currently understood to occur across the membrane of the digestive vacuole [27], and so the drug does not achieve intravacuolar concentrations which inhibit haematin dimerization. Since changes in sequence of vacuolar membrane protein PfCRT, crucially K76T, lysine to threonine, are convincingly linked to CQ-R in *P. falciparum* [28], which replaces a positively charged and polar by a neutral and hydrophobic residue, it is probable that efflux of polar, positively charged CQ2H+ is mediated through the modified protein. Other changes in PfCRT which also increase overall hydrophobicity of the protein, particularly of residues 72–76, are present in field CQ-R isolates. It is recognized that 4-aminoquinolines more hydrophobic than CQ, such as amodiaquine (AQ) and its metabolite mono-desethylamodiaquine (DAQ) retain some activity against CQ-R parasites [29]. This is believed to be due to their interaction with and retention in the hydrophobic lining of a CQ-R PfCRT channel [30–33]. Reversal of CQ-resistance *in vitro* by verapamil and activity of DAQ both vary with hydrophobicity of residues 72–76 of PfCRT [31]. Allelic replacement of a neutral by a positively charged residue at 76 or at some other positions in the PfCRT sequence effectively restores CQ-sensitivity and restores verapamil-insensitivity [33]. A reduction in vacuolar pH has been

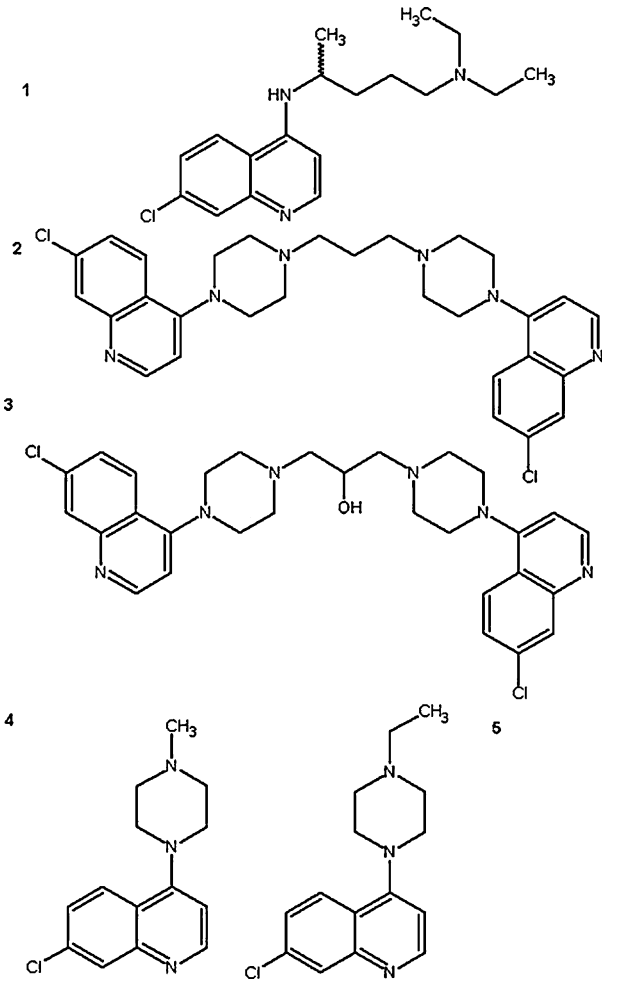

Fig. 1 – Structures of compounds used in the study. Chloroquine, showing asymmetric carbon atom (1), piperaquine (2), hydroxypiperaquine (3), cpd. 4, and cpd. 5.

associated with CQ-resistance, and in an alternative to the efflux theory, it has been suggested that aggregation of the haematin target under more acid conditions may reduce its binding to CQ [34]. The most recent work affords at present only equivocal support [22] for, or outright disagreement with [18] the haematin aggregation hypothesis. The *bis* 4-aminoquinolines PQ and OH-PQ probably, like CQ, also become concentrated within the vacuole, bind to haematin and inhibit its dimerization [3]. It remains to be determined how these agents retain their effects in CQ-resistant parasites.

The entry of a basic drug through lipid membranes and its distribution into the aqueous compartments of an infected erythrocyte is determined by lipid–water partition coefficient (expressed as log *P*) interacting with pH through the ionization constant(s) (pK_a) of the basic centre(s) of the drug. In order to understand drug action and resistance more fully we have therefore measured, in comparison with CQ, log *P* and pK_a values for PQ (**2**), OH-PQ (**3**) and two ''monomeric'' compounds, *N*-1′-(7-chloroquinolin-4-yl)-piperazines **4** and **5** representing halves of PQ (Fig. 1). We have modelled at equilibrium the aqueous and lipid distribution of the drugs in the parasitized erythrocyte to determine their expected accumulation ratios from plasma water (pH 7.4) through intraerythrocytic membranes and compartments into vacuolar water (vacuolar accumulation ratio: VAR) [35] and through vacuolar water into vacuolar lipid, lipid accumulation ratio (LAR). This confirms for CQ-S parasites, that while charged drug concentration in vacuolar water (VAR) increases as vacuolar pH decreases, the concentration of uncharged drug (base) in vacuolar membrane and other lipid sites in the digestive vacuole has a constant value for each individual drug, because the proportion of drug partitioned into lipid decreases as log *D* (the log of $[drug]_{lipid}/[drug]_{water}$ at equilibrium) decreases with reduced pH.

Activity of these agents in inhibition of haematin dimerization to β-haematin in a cell-free system (BHIA) has been determined, and also their potency against CQ-S and CQ-R *P. falciparum*, in comparison with CQ (**1**) itself.

We have also modelled the probable minimal energy conformations of the drugs in their protonated and unprotonated states using a semi-empirical quantum mechanical protocol [36], determining heats of formation and relevant structural features, which support conclusions based mainly on argument from physicochemical observations.

2. Materials and methods

2.1. Synthesis of new test substances

Compounds **4** and **5** were obtained from reaction of 4,7-dichloroquinoline with 1-methylpiperazine and 1-ethylpiperazine respectively, and were characterized by analysis, ^1H proton NMR and high-resolution mass spectroscopy (HRMS). Compound **4** has been previously prepared by another method [37], but its activity against malaria parasites was not reported.

2.1.1. *N-1′-(7-chloroquinolin-4-yl)-N-4′-methylpiperazine* 4

A solution of 4,7-dichloroquinoline (1 g, 5.05 mmol) in 1-methylpiperazine (30 mL, 0.270 mol) was heated to reflux for 4 h while monitoring the disappearance of starting material by TLC. Excess solvent was evaporated and the product purified via flash chromatography with silica gel. Elution with CH_2Cl_2/MeOH/Et_3N (95:4:1) gave pure **4** (1.12 g, 86% yield) as white crystals from methanol, mp 88–89 °C (lit. mp 86 °C). ^1H NMR ($CDCl_3$):δ 7.01–8.90 (5H) (Ar–H), δ 3.33 (s, 3H) (N–CH_3 boat), δ 3.18 (t, J = 3.9 Hz, 4H) (N–CH_2, 3′ and 6′), δ 2.62 (t, J = 3.9 Hz, 4H) ((N–CH_2, 2′ and 5′), δ 2.31 (s, 3H) (N–CH_3) (chair). HRMS calcd. For $C_{14}H_{16}ClN_3$ *m/z* 261.1033, found 261.1036 (M^+). The hydrochloride, prepared using methanolic HCl (10N), crystallized from methanol, mp 277–280 °C (dec.). Anal. Calcd. For [$C_{14}H_{16}ClN_3{\cdot}2HCl{\cdot}1H_2O$] C, 47.66; H, 5.67; N, 11.91; found C, 47.89; H, 5.84; N, 11.61%. [FW = 352.68].

2.1.2. *N-1′-(7-chloroquinolin-4-yl)-N-4′-ethylpiperazine* 5

Prepared in the same manner from 4,7-dichloroquinoline (5 g, 25.2 mmol) in 1-ethylpiperazine (150 mL, 1.17 mol) by refluxing for 6 h, the product **5** (6.36 g, 91% yield) crystallized from methanol, mp 82–83 °C. ^1H NMR ($CDCl_3$): δ 6.83–8.72 (5H) (Ar–H), δ 3.26 (t, J = 3.9 Hz, 4H) N–CH_2, 3′ and 6′, δ 2.74 (t, J = 3.9 Hz, 4H) N–CH_2, 2′ and 5′, δ 2.58 (q, J = 6.4 Hz, 2H) CH_2, δ 1.15 (t, J = 6.4 Hz, 3H) CH_3. HRMS calcd. For $C_{15}H_{18}ClN_3$ *m/z* 275.1189, found 275.1183. Anal. Calcd. For $C_{15}H_{18}ClN_3{\cdot}2H_2O$:C, 57.78; H, 7.06; N, 13.48. Found: C, 57.92; H, 7.18; N, 13.36%. The hydrochloride was prepared as above and crystallized from methanol, mp 288–289 °C (dec.). Anal. Calcd. for $C_{15}H_{18}ClN_3{\cdot}2HCl{\cdot}1H_2O$: C, 49.11; H, 6.00; N, 11.46. Found C, 48.89; H, 6.05; N, 11.31% [FW = 366.71].

The ^1H NMR spectrum of **4** showed that the piperazine ring exists in a dynamic equilibrium between the chair and boat conformers, as demonstrated by the appearance of a second *N*-methyl signal at 3.33 ppm (due to the magnetic de-shielding of the *N*-methyl group in the boat form by the magnetic cone of the adjacent benzene ring) in addition to the normal *N*-methyl resonance at 2.30 ppm arising from the chair conformer. As expected, in the doubly charged di-hydrochloride salt only the more stable chair form existed, with the N–CH_3 signal at 3.04 ppm. The corresponding ^1H NMR spectrum of the *N*-4′-ethyl analogue **5** also showed only the chair conformer to be present.

Samples of PQ were obtained from WHO (Dr. Piero Olliaro and Dr. Alan Shapiro) as the tetraphosphate tetrahydrate, while OH-PQ base was kindly supplied by Professor W. Peters. Racemic CQ diphosphate was from Sigma (UK).

2.2. Molecular modelling

For CQ, PQ, OH-PQ, **4** and **5**, protonated and base forms were modelled in HyperChem Release 7 for Windows (Hypercube Inc., Gainesville Florida) using the semi-empirical Austin method 1 (AM1) quantum-mechanical procedure [36]. Geometry was optimized to an RMS (root mean square) gradient of 0.001 *in vacuo*, [*cf* Ref. 23] (Polak-Ribière conjugate-gradient method). The optimized structure was then subjected to single-point computation using the AM1 programme in configuration-interaction, to find the total energies and heats of formation for the energy-minimized structures as bases and as the protonated cations (Table 1). Distances between the quinoline N-1 atoms and 4-amino N atoms, between bridging side-chain N atoms (in *bis* compounds), between quinoline N-1

Table 1 – AM1 geometrical optimization of compounds studied (energy in kcal mol^{-1}, distances in Å)

AM1 properties	R and S CQ	R and S CQ1H+	R and S CQ2H+	PQ	PQ2H+ (aromatic N)	PQ4H+	OH-PQ	OH-PQ2H+ (aromatic N)	OH-PQ4H+	**4**	**4** 2H+	**5**	**5** 2H+
Total energy	−84345	−84513	−84650	−141613	−141941	−142025	−149008	−149336	−149419	−69329	−69605	−72921	−73198
Heat of formation: *H*	23.65	170.2	347.9	126.7	428.8	974.0	81.25	383.1	929.4	62.71	416.3	57.15	410.4
Quinoline N-1 atoms (Å)	NA	NA	NA	17.65	18.29	18.30	17.53	18.23	18.36	NA	NA	NA	NA
Bridging side-chain N atoms (Å)	NA	NA	NA	4.985	4.965	5.073	4.932	4.944	5.073	NA	NA	NA	NA
Quinoline N-1 atoms and side-chain N atoms (Å)	7.893	7.999	8.991	6.526, 6.520	6.827, 6.819	6.830, 6.837	6.520, 6.512	6.795, 6.835	6.828, 6.835	6.514	6.852	6.466	6.816
Quinoline N-1 atoms and 4-amino (Å)	4.255	4.258	4.196	4.280, 4.280	4.202, 4.200	4.231, 4.231	4.280, 4.281	4.203, 4.198	4.231, 4.231	4.280	4.221	4.280	4.219
O–N (Å)	NA	NA	NA	NA	NA	NA	2.998, 3.136	2.980, 3.114	2.850, 3.079	NA	NA	NA	NA

The compounds are examined unionized (bases) and protonated. R and S CQ = rectus and sinister enantiomers of chloroquine base. PQ = piperaquine base. OH-PQ = hydroxypiperaquine base. **4** = compound **4** as base. **5** = compound **5** as base.

atoms (in *bis* compounds) and between quinoline N-1 atoms and side-chain N atoms (Table 1) were determined.

2.3. Physico-chemical properties

2.3.1. Role of ionization constant(s) and partition coefficient in the entry of drugs into cells

The accumulation of an ionizable drug in cells is determined (apart from special transport mechanisms) by two major parameters: the partition coefficient *P* between the aqueous and the lipid phase, usually expressed as log *P* (measured in the *n*-octanol-water system for the unionized compound), and its modification by the ionization constant(s) (pK_a) of the drug. For partially ionized compounds, the partition coefficient between aqueous and lipid phases at any fixed pH ($[drug]_{lipid}/[drug]_{water}$ at equilibrium) is called the distribution coefficient *D*, usually expressed as log *D*; this assumes that only the unionized base partitions from the aqueous to the organic phase [38]. The difference between log *P* and log *D* varies at different pH values because of the variation in the percentage of the drug ionized, and, for a drug with one basic centre, is obtained from the standard equation (1) for a base [39,40].

$$\log D = \log P - \log[1 + 10^{(pK_a - pH)}] \quad (1)$$

Thus it is possible [38,41] to calculate log *D* from observed log *P*, pK_a and pH.

As well as experimentally measuring log *P*, it is possible to estimate it using the *C* log *P* programme, developed by Hansch and Leo, although differences due to conformational isomerism are not taken into account [42]. Calculated values of log *P* were obtained for comparison using a modified commercial version of *C* log *P*, incorporated in version 7.0 of the Advanced Chemistry Development log *D* suite for Windows (Toronto, CANADA).

The ionized basic centres of compounds **1–5** can be described as: (a) the resonance-stabilised amidinium ion (made up of the N-1 of the quinoline and the amino group attached to C-4 of the same ring) and (b) a distal aliphatic protonated N-3. For CQ, **4** and **5**, which have one example of each centre, the correction needed in log *P* to obtain log *D* at a given pH involves the additive contribution of both ionized species, and the base Eq. (1) must be modified [43] to Eq. (2).

$$\log D = \log P - \log[1 + 10^{(pK_{a1} - pH)} + 10^{(pK_{a1} + pK_{a2} - 2pH)}] \quad (2)$$

Bis compounds PQ and OH-PQ are centro-symmetric and have two of each type of basic centre. Initial protonation at one basic centre may affect the other via a through-space electric effect of the now positively charged N ion on the other (uncharged) N atom, causing a slight reduction of the basicity of the second basic centre by inhibiting its protonation. The existence of four separate pK_a values for PQ and OH-PQ is therefore possible, and to provide for the contribution from all ionized species to the log *D*, the equation of Henderson and Hasselbach can be modified from Eqs. (2) and (3).

$$\log D = \log P - \log[1 + 10^{(pK_{a1} - pH)} + 10^{(pK_{a1} + pK_{a2} - 2pH)} + 10^{(pK_{a1} + pK_{a2} + pK_{a3} - 3pH)} + 10^{(pK_{a1} + pK_{a2} + pK_{a3} + pK_{a4} - 4pH)}] \quad (3)$$

Dissociation constants and partition coefficients were determined by Robertson Microlit Laboratories (Madison, NJ, USA) at 25 °C using the Sirius GLpK automated computerized

Table 2 – Physicochemical and other parameters for the compounds studied

Compound	pK_{a1}	pK_{a2}	pK_{a3}	pK_{a4}	log *P*	log $D_{7.4}$	log $D_{5.2}$	log $D_{4.8}$	$VAR_{pH\ 4.8}$	LAR	IC_{50} (nM) CQ-S (±S.E.)	IC_{50} (nM) CQ-R (±S.E.)	IC_{50} Res/Sens	BIHA IC_{50} ±S.D. (*n*)
1 CQ	10.18[c]	8.38[c]	–	–	4.72[c]; 4.69[d]	0.96[c]; 0.92[a]	−3.44[c]; −3.44[a]	−4.24[a]	143482[f]; 143482[e]	9.1[g]; 8.25[h]	23.4 (±0.21)	329 (±9.00)	14.1	1.30 ± 0.30 (8)
2 PQ	6.88	6.24	5.72	5.39	6.11; 6.16[d]	5.99; 5.99[b]	2.41; 2.41[b]	0.97[b]	104378[f]; 104378[e]	977237[g]; 973492[h]	19.9 (±2.01)	49.0 (±1.79)	2.46	0.62 ± 0.12 (6)
3 OH-PQ	6.60	6.41	5.39	4.83	5.67; 6.38[d]	5.15; 5.60[b]	2.11; 2.54[b]	1.30[b]	19874[f]; 19874[e]	141254[g]; 398118[h]	41.6 (±16.6)	62.4 (±6.70)	1.50	0.58 ± 0.21 (6)
4	7.63	5.42	–	–	3.02; 2.92[d]	2.26; 2.59[a]	0.10; 0.17[a]	−0.52[a]	1287[f]; 1287[e]	182[g]; 386[h]	2485 (±371)	>5000	NA	3.80 ± 1.20 (6)
5	7.92	5.54	–	–	3.48; 3.46[d]	2.35; 2.84[a]	0.21; 0.26[a]	−0.45[a]	1966[f]; 1966[e]	224[g]; 693[h]	2213 (±330)	4486 (±670)	2.03	3.35 ± 0.94 (8)

CQ-S: T996, CQ-sensitive clone. CQ-R: K1, CQ-resistant strain. Results from two experiments in triplicate. BIHA = β-haematin inhibition assay. NA = not applicable.

[a] Calculated from Eq. (2).
[b] Calculated from Eq. (3).
[c] From Ref. [68].
[d] From ACD programme.
[e] Calculated from equations in Refs. [35,49].
[f] Eq. (4): antilog(calc log $D_{7.4}$ − calc log $D_{4.8}$).
[g] Eq. (5): antilog obs log $D_{7.4}$.
[h] Eq. (5): antilog calc log $D_{7.4}$.

potentiometric system [44] which is capable of resolving ionization constants of multiprotic substances. Titration employed water containing 0.15 M KCl (representing a physiological concentration of positive and negative counter-ions) in an argon atmosphere. The pK_a values were determined in triplicate with a S.E. of ±0.20. For PQ and OH-PQ the base precipitated above pH 7.0. The titrations were therefore carried out with methanol as a co-solvent, using five different ratios of methanol to water. The aqueous pK_a was determined by extrapolation to 0% methanol using the method of Yashuda-Shedlovsky [45,46] which gives a linear fit. log *D* values at the physiological pH of 7.4 and at pH 5.2, an early reported pH for the digestive vacuole [17], were estimated from the experimental plot of log *D* versus pH. We compared these reported values with log *D* values we calculated from log *P* and pK_a using Eq. (2) [43] and Eq. (3) [47]. It should be noted that in Eqs. (2) and (3), $pK_{a1} > pK_{a2} > pK_{a3} > pK_{a4}$.

Partition coefficients between octanol and water were measured by dual-phase potentiometric titration using various amounts of water-saturated *n*-octanol. Titrant addition was carried out with vigorous stirring of the assay solution. Three different ratios of octanol/water were employed for each compound. The log *P* values were obtained from the difference between the aqueous pK_a of the species and the apparent pK_a determined from the dual phase titration. Measurements were carried out in triplicate with a S.E. of ±0.40. The potentiometric method was validated by comparison with results obtained by the standard shake-flask technique [48]. We have also reported the values of log *P* for the unionized bases calculated by the ACD log *D* programme (Table 2).

2.3.2. *Vacuolar accumulation ratio (VAR)*

Since the vacuolar (lysosomal) pH is being regulated to an acidic value within the malaria parasite, providing optimal conditions for haemoglobin digestion [17,34,18] the potential vacuolar accumulation ratio for a drug (VAR) into intravacuolar water for a drug with one basic centre protonated may be calculated using the ratio of proton concentration in the aqueous contents of the vacuole to that in the aqueous medium (pH 7.4) external to the cell.

Applying the Henderson–Hasselbach equation to measured pK_as, it is possible to calculate accumulation ratios from plasma (pH 7.4) to the vacuole (vacuolar accumulation ratios: VAR) at any specified vacuolar pH for CQ with two protonatable basic centres [35] and for *bis*-quinolines with four centres [49]. However, if log *D* values have been calculated already, using observed log *P* and pK_a, the log of VAR at any vacuolar pH is easily obtained by subtracting log *D* at the proposed vacuolar pH, from log *D* at pH7.4 since log *P* is automatically eliminated from the calculation [Eq. (4)]. If calculated log *D* values are used, VAR values identical to those obtained from the equations of Krogstad and Schlesinger [35] and Rykebusch et al. [49] are produced. With observed values of log *D*, results may differ slightly (Table 2). In view of the high degree of agreement between observed and calculated VARs, and the utility of being able to calculate a log *D* for any vacuolar pH value, we used for analysis the log *D* values calculated from Eqs. (2) and (3) throughout the study.

Observed log *D* values at pH 7.4 and pH 5.2 are also reported in Table 2.

$$\text{VAR} = \text{antilog}(\log D_{(\text{pH}\,7.4)} - \log D_{(\text{pH}_v)}) \quad (4)$$

where pH_v is vacuolar pH. It is important to recognize that this calculation only refers to charged drug in the aqueous phase, taking into account that 61% CQ in plasma is protein-bound in healthy persons [50]. This is likely to be higher for PQ and OH-PQ, because of their higher hydrophobicity (compare quinine where the log $D_{7.4}$ is 1.96 [51] compared with 0.92 for CQ, and the protein binding is 92.8% [52]). In addition the digestive vacuole contains variable amounts of parasite protein and of haemoglobin at different stages of digestion.

2.3.3. *Lipid accumulation ratio (LAR)*

Modelling of the equilibrium drug distribution between different compartments of the infected erythrocyte revealed that, although the proportion of an unprotonated basic drug which entered lipid from the aqueous phase increased with pH (examined between pH 4.8 and 7.4), the actual concentration in lipid did not vary between erythrocyte membrane, parasite membrane, vacuole membrane and intravacuolar lipid.

$$\text{LAR} = \text{VAR}(\text{antilog}\log D_{(\text{pH}_v)})$$

$$\log \text{LAR} = (\log D_{(\text{pH}\,7.4)} - \log D_{(\text{pH}_v)}) + \log D_{(\text{pH}_v)}$$

when pH_v 7.4, log LAR = log $D_{(\text{pH 7.4})}$; when pH_v 4.8,

$$\log \text{LAR} = (\log D_{(\text{pH 7.4})} - \log D_{(\text{pH 4.8})}) + \log D_{(\text{pH 4.8})}$$

$$\log \text{LAR} = \log D_{(\text{pH}\,7.4)} \quad (5)$$

Thus, for any basic drug present at concentration 1 nM in extracellular water at pH 7.4, LAR in the external membrane is antilog (log $D_{(\text{pH 7.4})}$) nM. As pH of an internal aqueous vacuole is lowered from 7.4, the increase in log VAR due to proton trapping and decrease in log *D* at lower pH in the vacuolar water ensures drug distribution into vacuolar lipid remains constant at antilog (log $D_{(\text{pH}7.4)}$) nM [53].

2.3.4. *Comparison of intravacuolar with extracellular pH changes*

The insensitivity to variations of vacuolar pH of LAR contrasts with its sensitivity to pH changes in the aqueous medium surrounding the infected erythrocyte. When the medium pH is changed, a rise from pH 7.4 to 7.6 more than doubles the concentration of charged CQ (CQ2H+) VAR in vacuolar water, and of CQ in the erythrocyte lipid/membrane phase (LAR), and, according to our calculations (*cf* [53]), throughout lipid in the parasite/host cell complex, including the vacuole membrane and lipid droplets, while a further rise in plasma pH to 7.7 almost doubles VAR and LAR again. The concentration change in vacuolar lipids follows from increases of the same order in CQ2H+ concentration in the vacuolar water, without vacuolar pH alteration. Conversely, decreasing medium pH from 7.4 to 7.2 more than halves CQ concentration in the vacuolar lipid, and CQ2H+ in the vacuolar water.

The reduction of CQ activity against cultured *P. falciparum* on lowering medium pH and enhancement with higher pH was discovered by Yayon et al. [54] and has been confirmed several times. This situation can be modelled well using Eqs. (4) and (5) (above). Raising external medium pH to 7.6, while maintaining vacuolar pH will give a greater value for (log $D_{(\text{pH 7.6})}$ − log $D_{(\text{pH 4.8})}$) and thus a greater antilog or VAR. At the same time, because of the higher log *D* at pH 7.6, LAR, its antilog, will be greater.

The discovery of the influence of medium (plasma) pH on the availability of CQ to the intraerythrocytic malaria parasite [54] appears of possible interest in malaria treatment because lactic acidosis (blood pH value $\leq$7.3 with a venous blood lactate concentration $\geq$5 mM) where blood pH can be as low as 7.14 [55], is a frequent complication of severe falciparum malaria and an independent predictor of death [56]. With a plasma CQ concentration similar to that at pH 7.4, a blood pH of 7.1 might lead to a 3.79-fold reduction in VAR and LAR and a consequent decrease in antiplasmodial efficiency.

2.3.5. *Calculation of percentage of molecules with a basic centre ionized, from pH and pK_a*

The equation given by Adrien Albert [57] was used for each basic centre:

$$\text{ionized}\,(\%) = \frac{100}{1 + 10^{(\text{pH}-\text{pK}_a)}} \quad (6)$$

An ExCel chart was prepared, and results, rounded to one place of decimals, are given in Table 4.

2.4. *β-Haematin inhibitory activity (BHIA)*

This test, in pH 5.0 buffer containing acetate as a phase-transfer catalyst [58], was modified from that described by Parapini et al. [59] by use of pyridine to ensure the final OD values conformed more closely with the Beer–Lambert law (haematin, which tends to aggregate in aqueous solution, was converted into the pyridine haemichrome to ensure that the law was obeyed [60]). One hundred microliters of each stock drug solution was added to wells in row A of a 96-well microtitre plate, except for the negative control well A12 to which 100 μL of distilled water was added. [Stock solutions of drugs were prepared in water at 40 mM (solubility was helped where needed by titration with HCl). PQ as the tetraphosphate tetrahydrate was dissolved in warm water while base OH-PQ was dissolved in warm water using 0.1N HCl. Compounds **4** and **5**, crystalline dihydrochloride monohydrates, were dissolved in warm water. Chloroquine was used as the commercial diphosphate in water.] In rows B to H, 50 μL distilled water was distributed using a multipipette. Then 50 μL was withdrawn from wells in row A and mixed with wells in row B. Serial dilution of 50 μL from wells in row B into wells in row C was carried on until row H whence 50 μL was discarded. Fifty microliters of 8 mM haemin chloride in DMSO was added to each well in the plate, using the multipipette without touching the well contents. From row H upwards, 100 μL of 8 M acetate buffer was added to each row including row A. [Acetate buffer pH 5.0. Solid sodium acetate was made up to 8 M with warm water (continue to heat at 37 °C in a water bath while mixing: it will not dissolve completely) and then the pH was adjusted to 5.0 with 8 M acetic acid at 37 °C, which led to the remaining solid dissolving]. The contents of each well were individually mixed, starting from row H and proceeding to row A using a multipipette set at 200 μL. The experiment was incubated at 35 °C for 24 h. [The final DMSO

concentration during the incubation was 25% (w/v), while final haematin concentration (0.4 μmol/200 μL well) was 2 mM, and the highest final drug concentration used was 10 mM, a top drug/haematin molar ratio of 5:1].

To harvest the experiment, 1 mL DMSO was added to a series of Eppendorf 1.5 mL centrifuge tubes to match the arrangement of the microtitre plate. Using the DMSO, the content of each well was washed and mixed into its centrifuge tube and incubated for 30 min at 35 °C. The tubes were then centrifuged in a swing-out rotor for 20 min at 3000 × *g*. The closure was removed from each tube in a rack and, ensuring each was well seated, the rack inverted once to discard the supernatant, draining on absorbent towels. To the sediment in each tube 1 mL NaOH was added, then incubated 30 min at 35 °C, and the contents of each tube washed and mixed into 1 mL aqueous 5% (v/v) pyridine in a microcuvette.

Absorption (optical density) of each cuvette was read in visible light at 414 nm.

Assuming the mean absorption of the drug-free control cuvettes is 100%, the relative % inhibition of the β-haematin formation [100 − ((OD test/mean OD control) × 100)] by different concentrations of drug was calculated. Percentage inhibition values were normalized against the maximum inhibition (assumed 100%) produced by CQ, and the drug:haematin molar ratios for 50% inhibition were obtained by regression analysis of the linear part of the sigmoid curve.

2.5. *Drug activity tests against P. falciparum*

Drugs were tested at least twice in triplicate for ability to inhibit the proliferation of a chloroquine-resistant (K1) isolate and a chloroquine-sensitive (T9-96) cloned isolate of *P. falciparum*, from Kanchanaburi and from Mae Sod, Thailand, respectively [61,62], cultured *in vitro*, using a [^{3}H] hypoxanthine incorporation procedure [63].

Briefly, the parasites were grown in A+ human erythrocytes, with 10 mL AB serum (National Blood Service, UK) added per 100 mL RPMI medium. Before use for drug assay, parasites were synchronized twice using sorbitol lysis [64]. An initial 1% parasitaemia at 5% haematocrit, with >95% of parasites in the growing young trophozoite stage was prepared. After preparation of stock drug solutions in serum-free medium, serial dilutions were prepared in 96-well flat-bottomed microtitre plates and then an equal volume of the infected blood suspended in medium was added to give a final 2.5% haematocrit at 1% parasitaemia. After incubation in a sealed vessel with 3% O_2, 4% CO_2, 93% N_2 at 37 °C for 24 h, [^{3}H] hypoxanthine, of specific activity 611 GBq (16.5 Ci)/mmol (Amersham, UK) was added as 10 μL of a 20 μCi/mL solution to each well, re-gassed and incubated for a further 18–24 h. Red cells were harvested from each well (Filtermate 196, Packard: Perkin Elmer Life Sciences, Boston, USA) on to Unifilter 96-well plates (Packard) followed by water washing for lysis, removal of unincorporated isotope and of other soluble components. After drying at 56 °C, the undersides of the plates were sealed and scintillation fluid added to each well before sealing the top of the plate. Tritium disintegrations per minute (dpm) were determined in a Packard 'Topcount' scintillation spectrometer, and the data were collected on a floppy disc. Percentage inhibitions of incorporation were calculated using the following equation: % inhibition = 100 − [((dpm test − mean dpm uninfected cells)/(mean dpm infected cells − mean dpm uninfected cells)) × 100].

These values were used to plot dose–response curves from which the IC_{50} values were derived by non-linear regression analysis (Microsoft EXCEL—add-in XL-fit program, ID Business solutions, Guildford, UK). Mean, standard error and 95% confidence intervals were calculated.

3. Results

3.1. *Molecular modelling (Table 1 and Figs. 3–7)*

3.1.1. *R- and S-CQ*

CQ **1** has a side chain asymmetric C atom (see Figs. 1 and 3), and commercial supplies are racemic, so both *R* and *S* enantiomers were modelled. The AM1, restricted Hartree-Foch calculations (25 °C) carried out in the present study confirm that the *R* and *S* forms are true enantiomers and energetically identical in all respects, as was demonstrated in lanthanide NMR studies of the base in acetone at 20 and 48 °C carried out by Angermann et al. [65]. We have used the coordinates, kindly supplied by Dr. Angermann, to make text files for the three-dimensional solution structures, and modelled them first in the *.ent and then in the *.hin Hyperchem formats (not shown). Although these authors found a close hydrophobic association between the side-chain and aromatic ring at 20 °C, at 48 °C their structure for the base bears a very close resemblance to our calculated 25 °C *in vacuo* minimal energy conformation (Fig. 3). The side chain extends to one side and above the aromatic ring. The authors suggest the ''unusual buckling'' of the side chain in solution at both temperatures may be due to an intramolecular dipole-induced dipole type of interaction between the relatively positive N-3 ethyl groups and the π-electron system of the quinoline ring. While their 20 °C N-1 to N-3 distance was 7.39 Å, at 48 °C it was 9.33 Å. Our (25 °C) calculated estimate is 7.893 Å which is comparable and intermediate. In the earlier X-ray crystallographic study of CQ diphosphate, representing the diprotonated form, the N-1 to N-3 distance was found to be 14.1 Å [66]. Here, electrostatic repulsion between the positive charges of protonated N-1 and N-3 and interaction with the phosphate groups stabilizes an extended form. In our models of CQ, the greatest distance between protonated quinoline N-1 and aliphatic protonated N-3 was 8.991 Å and appreciably less (7.999 Å) in the monoprotonated form, with the side-chain still somewhat buckled in both cases, indicating that an apparent attraction to the quinoline π-electron system can still be recognized in the diprotonated form.

In the calculated models a change in the distance from N-1 to secondary 4-amino N-2 on protonation of the aromatic N-1 was also of interest. Both enantiomers showed a marked shortening of this dimension from 4.255 (base) and 4.258 (protonated aliphatic N-3) to 4.196 Å in the diprotonated species, supporting the formation of the strongly resonance-stabilized aromatic amidinium ion.

3.1.2. *Compounds* **4** *and* **5**

The features of the aromatic amidinium ion differed from that of CQ and resembled PQ and OH-PQ (below), with an N-1 to N-2 separation of 4.221 Å in the diprotonated form of **4** compared with 4.280 Å in the base, and 4.219 compared also with 4.280 Å for **5** (*cf* CQ, 4.196 compared with 4.255 Å).

3.1.3. *PQ*

The minimal energy structure for PQ (**2**) was extended, with a distance between the quinoline N-1 atoms for the tetraprotonated form of 18.29 Å. The mean N-1 to N-2 separation in the aromatic amidinium ions in the diprotonated species was 4.201 Å (*cf* CQ, 4.196 Å), reduced from 4.280 in the base, supporting the base-weakening of the amidinium compared with CQ noted in physicochemical measurements (below). The distance increased to 4.231 Å when the final two piperazine N atoms had been protonated.

3.1.4. *OH-PQ*

The calculated heat of formation of OH-PQ (**3**) was appreciably lower than for PQ by 45.45 kcal mol^{-1}, which may perhaps be accounted for by weak internal hydrogen bonding between the hydroxyl group and one or both of the bridging piperazine N atoms (minimal O–N distance in the protonated species of 2.850 Å). This was also suggested as a result of the physicochemical study (below). The features of the amidinium ion in OH-PQ, and the characteristics of the minimum energy structure were similar to those of PQ.

3.1.5. *Relative orientation of the quinoline and piperazine rings*

The minimum energy orientation of the piperazine rings in **4**, **5**, PQ and OH-PQ, was similar, probably influenced by the proximity of the quinoline C-5 proton. This resulted in the ''plane'' of the piperazine ring being twisted relative to that of the quinoline, agreeing with the NMR study on **4** and **5** and supporting a cause for the base-weakening effect as suggested in the physicochemical study (below).

3.2. *Physicochemical properties (see Tables 2, 3A and 3B)*

The dissociation constants, log *P* values, log *D* values, estimates of VAR at pH 4.8 and 5.2, and LAR values for cpds. **1–5** are shown in Tables 2, 3A and 3B. The log *P* values calculated from the drug structures by the ACD programme closely approximate to the measured values. In addition, log *D* values for pH 7.4 and 5.2 calculated from measured values of log *P* and pK_a using Eqs. (2) or (3) are close to the measured values. The VAR derived from the calculated estimates of log *D* from Eqs. (2) or (3) is invariably identical to the VAR value calculated from equations reported earlier [35,49] (Table 2). Although for CQ (two relevant protons) the logarithmic relationship between VAR and vacuolar pH very closely approximates linearity, it is not inherently linear, rather a second order polynomial while for **4** and **5** (two protons) and PQ and OH-PQ (four protons) the curve is clearly seen to be concave (see Fig. 2).

3.2.1. *Acid dissociation constants (pK_a) (see Table 2)*

In the parent compound 4-amino-7-chloroquinoline, and in the similarly constituted CQ, protonation occurs at the quinoline ring N-1 to form a planar resonance-stabilized 1,4-amidinium ion with measured pK_a values of 8.23 and 8.38 respectively [67,68]. However, in the (*N*-1′-quinolin-4-yl)-*N*-4′-alkylpiperazines **4** and **5**, the N attached to the 4-position of the quinoline ring is also the N-1′atom of a piperazine ring, making the substitution spatially equivalent to a tertiary dialkylamino group. The effect of steric hindrance with the adjacent quinoline C-5 proton causes the dialkylamino moiety to be twisted out of the plane of the quinoline ring, and this departure from co-planarity diminishes the resonance stabilization of the planar amidinium ion. This base-weakening effect is shown in going from 4-aminoquinoline (pK_a 9.08) [69] to 4-dimethylaminoquinoline (pK_a 8.36) [70] and allows the pK_{a1} values of (**4**) (7.63) and (**5**) (7.92) to be identified with the aromatic amidinium ion. Therefore the pK_{a1} and pK_{a2} values of PQ and OH-PQ between 6.41 and 6.88 also belong to the aromatic amidinium ions.

With respect to the protonatable aliphatic tertiary amine groups in compounds **2–5**, while the pK_{a1} for piperazine itself is 9.81, pK_{a2} for the second N is lowered to 5.55 due to the unit positive charge on N-1 [71]. The same explanation accounts for pK_{a2} in **4** (5.42) and **5** (5.54) (N-4′) and for the pK_{a3} and pK_{a4} values of PQ (**2**) and OH-PQ (**3**), (where there is one for each of the piperazine rings).

Results of the potentiometric titrations of PQ confirm that stepwise protonation occurs, with pK_{a1} and pK_{a2} values of 6.88

Table 3A – Vacuolar accumulation ratio (VAR) and lipid accumulation ratio (LAR) values for CQ at vacuolar pH from 4.8 to 7.4

CQ concentration in plasma (nM) (assumed constant)	Vacuolar pH (pH_v)	[CQ] in vacuolar water (nM) (VAR) (Eq. (4))	[CQ] in lipid (nM) LAR (Eq. (5))	log *D* (pH_v)
1.0	4.8	143482	8.25	−4.24
1.0	5.0	57130	8.25	−3.84
1.0	5.2	22749	8.25	−3.44
1.0	5.4	9060	8.25	−3.04
1.0	5.6	3609	8.25	−2.64
1.0	5.8	1438	8.25	−2.24
1.0	6.0	573	8.25	−1.84
1.0	7.4	1	8.25	0.917

The last column shows the calculated log *D* values determining the VAR and LAR for each pH. *Note*: no change in LAR with pH (assuming the parasite is CQ-sensitive).

Table 3B – Comparison of VAR and LAR values at vacuolar pH 4.8 for a series of nine 4-amino, 7-chloroquinoline drugs

Drug	Vacuolar pH	[Drug] in vacuolar water (nM) (VAR) (Eq. (4))	[Drug] in vacuolar lipid (nM) (LAR) (Eq. (5))	log *D* (pH 4.8)	log *D* (pH 7.4)	Resistance index
DECQ	4.8	144114	0.56	−5.41	−0.251	36.66
HCQ	4.8	139607	4.46	−4.50	0.650	79.12
CQ	4.8	143482	8.25	−4.24	0.917	14.10
DAQ	4.8	89366	40.8	−3.34	1.61	5.39
AQ	4.8	47410	666	−1.85	2.82	1.98
PQ	4.8	104378	973492	0.97	5.99	2.46
OH-PQ	4.8	19874	398118	1.30	5.60	1.50
Cpd **4**	4.8	1287	386	−0.524	2.59	NA
Cpd **5**	4.8	1966	693	−0.453	2.84	2.03

Calculated log *D* values at pH 4.8 and 7.4 are included together with the resistance index (RI) (IC_{50} nM of drug against CQ-R parasite/IC_{50} nM drug against CQ-S parasite) for each drug.

and 6.24 for the two aromatic amidinium ions, and pK_{a3} and pK_{a4} of 5.72 and 5.39 for the distal tertiary N-4′ of the two piperazines. Very similar numbers for the amidinium ions were obtained for the analogue OH-PQ (pK_{a1} 6.60 and pK_{a2} 6.41) where a slight base-weakening effect for the piperazine N-4′ (pK_{a3} 5.39 and pK_{a4} 4.83) similar to the drop from triethylamine to diethylaminoethanol [72] was seen, probably due to hydrogen bonding of the –OH group with one or other of the adjacent tertiary N-4′ atoms.

3.2.2. *Experimental log P values (see Table 2)*

The anticipated enhanced lipophilic properties of the *bis*-quinolinyl compounds PQ and (OH-PQ) were revealed by the extraordinarily high measured values of log *P*, with experimental numbers of 6.11 and 5.67 in reasonable agreement with calculated ACD log *P* values. Compounds **4** and **5** gave experimental log *P* values in excellent agreement with those calculated using the ACD suite (Table 2), with the expected increase in log *P* due to the larger alkyl group in **5**.

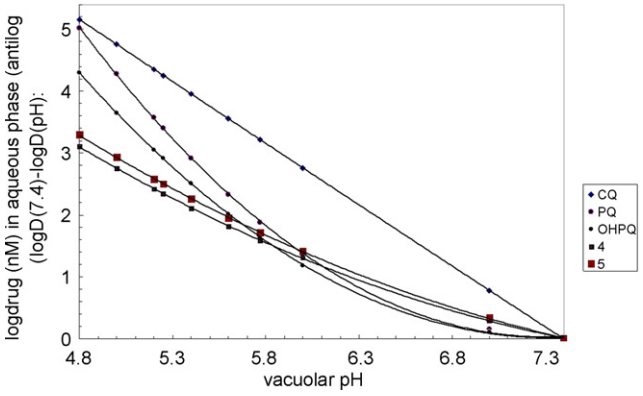

Fig. 2 – Graph showing the inverse relationship between vacuolar pH (*x*) and log VAR (*y*) for CQ (chloroquine), PQ (piperaquine), OH-PQ (hydroxypiperaquine), cpd. 4 and cpd. 5. Second order polynomial equations for the graphs, as follows: CQ: $y = 0.0058x^2 - 2.0611x + 14.917$ ($R^2 = 1$); PQ: $y = 0.8019x^2 - 11.706x + 42.75$ ($R^2 = 0.9997$); OH-PQ: $y = 0.67x^2 - 9.8233x + 36.016$ ($R^2 = 0.9999$); 4: $y = 0.2251x^2 - 3.9346x + 16.801$ ($R^2 = 0.9999$); 5: $y = 0.2197x^2 - 3.9387x + 17.127$ ($R^2 = 0.9999$).

3.2.3. *pH-modulated log D values (see Tables 2, 3A, 3B and 4)*

3.2.3.1. *Chloroquine.*

At physiological pH (7.4) the proportion of molecules positively charged is 99.8%, while 90.5% are doubly protonated, 2+ (90.5% of the quinolinium N-1 and 99.8% of the relevant tertiary aliphatic N-3) (Table 4). This results in a calculated log *D* value of 0.92 giving a LAR (antilog of $\log D_{(pH\ 7.4)}$) from the blood plasma to the RBC lipid membrane of 8.25 (membrane concentration is 8.25 times the plasma concentration).

At vacuolar pH (4.8), 100.0% of the molecules are doubly positively charged (2+) (Table 4). The log *D* value is −4.24, and while the membrane transfer ratio from the vacuolar content to the vacuolar membrane is extremely low, the VAR into vacuolar water, calculated from log *D* values is extremely high at 143,482. Hence the overall LAR from plasma into vacuolar lipid phase is found to be identical to the value reported above for the RBC membrane (8.25). This feature is maintained throughout the pH range (4.8–7.4) studied (Table 3A): the lipid concentration in vacuolar membrane and enclosed lipid remains constant as pH (and log *D*) decrease because of the increase in VAR in vacuolar water.

3.2.3.2. *Compounds 4 and 5.*

At physiological pH, only 1.0 and 1.4% of molecules of compounds **4** and **5** are 2+ (quinolinium and aliphatic piperazine N-4′ [N3]) (Table 4). This results in log *D* values of 2.59 and 2.84, giving LARs from the blood plasma to the RBC lipid membrane of 386 and 693.

At vacuolar pH (4.8), 80.7 and 84.6% of molecules of **4** and **5** are 2+ (Table 4). Their log *D* values are −0.52 and −0.45 while the VAR values in vacuolar water are very low, at 1287 and 1966. LARs from the blood plasma or medium through vacuolar water to the vacuolar lipid are identical to those in the RBC membrane.

3.2.3.3. *PQ and OH-PQ.*

Due to lower pK_a values, these are only 6.5 and 9.3% doubly charged (first and second quinolinium N-1), and 1.0% and 0.3% 4+ (2 quinolinium N1 and 2 aliphatic piperazine N-4′ [N3]) at pH 7.4 (Table 4). Thus the log *D* values remain very high, 5.99 and 5.60, similar to their log *P* values, corresponding to huge LARs from the blood plasma to the RBC lipid membrane of 973,492 and 398,118, respectively, nearly six orders of magnitude higher than CQ. At vacuolar pH (4.8), PQ and OH-PQ are 96.5 and 97.6% 2+, and 79.6 and 51.7% 4+ (Table 4). This is reflected in the drop in their

Table 4 – The percentage of molecules of CQ, PQ, OH-PQ, 4 and 5, singly or multiply protonated (H+) at pH 7.4 and 4.8, calculated from the pK_a values by Albert's equation [57]

Drug and amino N		pH	pK_a	% 1H+	% 2H+	% 3H+	% 4H+	pH	pK_a	% 1H+	% 2H+	% 3H+	% 4H+
CQ	N3	7.4	10.18	99.8				4.8	10.18	100.0			
CQ	N1	7.4	8.38		90.5			4.8	8.38		100.0		
PQ	N1	7.4	6.88	23.2				4.8	6.88	99.2			
PQ	N1	7.4	6.24		6.5			4.8	6.24		96.5		
PQ	N3	7.4	5.72			2.1		4.8	5.72			89.3	
PQ	N3	7.4	5.39				1.0	4.8	5.39				79.6
OH-PQ	N1	7.4	6.6	13.7				4.8	6.6	98.4			
OH-PQ	N1	7.4	6.41		9.3			4.8	6.41		97.6		
OH-PQ	N3	7.4	5.39			1.0		4.8	5.39			79.6	
OH-PQ	N3	7.4	4.83				0.3	4.8	4.83				51.7
4	N1	7.4	7.63	62.9				4.8	7.63	99.9			
4	N3	7.4	5.42		1.0			4.8	5.42		80.7		
5	N1	7.4	7.92	76.8				4.8	7.92	99.9			
5	N3	7.4	5.54		1.4			4.8	5.54		84.6		

log *D* values to 0.97 and 1.30 while the VAR values in vacuolar water are large at 104,378 and 19,874. LARs from the blood plasma through vacuolar water to the vacuolar lipid, identical to RBC membrane values, are huge.

3.3. *β-Haematin inhibitory activity (BHIA)*

CQ had an IC_{50} molar ratio versus haematin of 1.30, while those of **4** and **5** were 3.8 and 3.35, about 1/3 as active as CQ. PQ and OH-PQ had molar ratios of 0.62 and 0.58, about twice as active as CQ. The molar ratios of **4**, **5**, PQ and OH-PQ were each significantly different from that of CQ (see Table 2).

According to literature reports, many 4-amino-7-chloroquinolines are active in the BHIA cell-free system, with drug:haematin molar ratios of 4 to 5, but only a small selection are active antiplasmodials. The probable reason, bearing in mind the digestive vacuole target in intraerythrocytic malaria parasites [15], is that a significant VAR is essential [16,17,20,21] for high antiplasmodial activity. For an optimal concentration within the vacuole, the 4-aminoquinoline drug structure requires at least two basic nitrogen atoms with suitable pK_a values [16,35]. After the initial concentration step from external pH 7.4 to vacuolar pH 4.8, (143,482 times for CQ) (see Tables 2, 3A and 3B), specific haematin/CQ binding [13] takes place with an association constant (measured in 40% DMSO) of 5.52 (dissociation constant 3 μM) [58], which prevents detoxication of haematin to insoluble crystals of the haematin head to tail cyclic dimer or β-haematin [19]. The careful study of Parapini et al. using BHIA [59] indicates a CQ IC_{50} value of 1.39–1.65 haematin molar equivalents, similar to the value of 1.3 we have observed here, while Egan [58] reports a 1:1 stoichiometry in 40% DMSO. The PQ and OH-PQ molar concentration equivalent to haematin is half that of CQ, suggesting that each of the 4-amino-7-chloroquinoline moieties in these *bis*-quinolinyl drugs binds to one iron porphyrin molecule. This probability is supported by molecular modelling of the minimum-energy conformation of PQ and OH-PQ which shows that the quinoline rings are well separated and relatively unhindered (above).

3.4. *Drug tests in vitro against P. falciparum (Table 2)*

PQ (**2**) was as potent as CQ (**1**) against the CQ-sensitive T996 parasite, but in the CQ-resistant K1 parasite the IC_{50} was only 2.46 times higher, that is the ''Resistance Index'' (RI) was 2.46 as opposed to 14.1 for CQ. The potency of OH-PQ (**3**) was slightly lower in both parasites and RI was 1.5. However, both half-PQ compounds, **4** and **5**, had very low potency in CQ-S, with a potency value against CQ-R measurable only for **5**. RI was however 2.03 (see Table 2). IC_{50} of **4** for K1 was not reached at the drug concentrations tested.

4. Discussion

4.1. *Molecular modelling*

4.1.1. *Possible pharmacophore for haematin binding*

Support was given by the molecular modelling study to conclusions from physicochemical observations. In addition, modelling the minimal energy structures in **1–5** (Figs. 3–7) revealed a common relatively unhindered planar area consisting of the 4-amino-7-chloroquinoline moiety which, in the case of CQ included the asymmetric –CH (with its methyl carbon) attached to N-2, and in PQ, OH-PQ, **4** and **5** one of the methylene carbons attached to the piperazine N-1′ in an equivalent position. In PQ and OH-PQ the second 4-amino-7-chloroquinoline moiety is also in a suitable position to bind to haematin and presents an essentially identical picture (Figs. 3–7). A disturbing diversity of structures for the 4-aminoquinoline/haematin complex has been proposed, most of which rely on analysis of interaction with the oxo-dimer form, predominant in neutral and aqueous solution [e.g. 73,74]. More consistent and satisfying results may be achieved by considering interaction with monomeric haematin as seen under

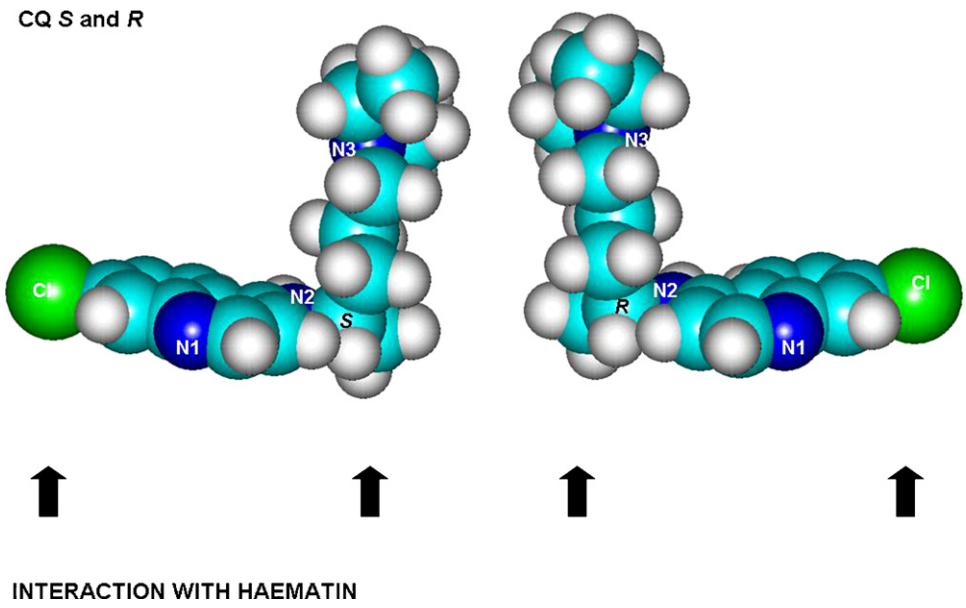

Fig. 3 – Calculated models of *S*- and *R*-CQ base using AM1. In each enantiomer the aromatic heterocyclic area likely to interact with haematin is indicated. (Colours: C = light blue (unlabelled), H = grey (unlabelled), N = dark blue (labelled N1, N2 and N3), Cl = green (labelled Cl)). (For interpretation of the references to color in this figure legend, the reader is referred to the web version of the article.)

acidic conditions [75,58]. Egan and colleagues recently reported [23] the haematin dimer (β-haematin) can be formed in association with the long-chain neutral lipid *n*-octanol under acid conditions. The lipophilic pre-dimer structure proposed for haematin (ferriprotoporphyrin IX–H_2O with undissociated propionic acid groups) [23] appears suitable for ring-ring interaction with a 4-amino-7-chloroquinoline pharmacophore, in the lipid or in the aqueous phase before transfer to the lipid, which would prevent the dimerization reaction.

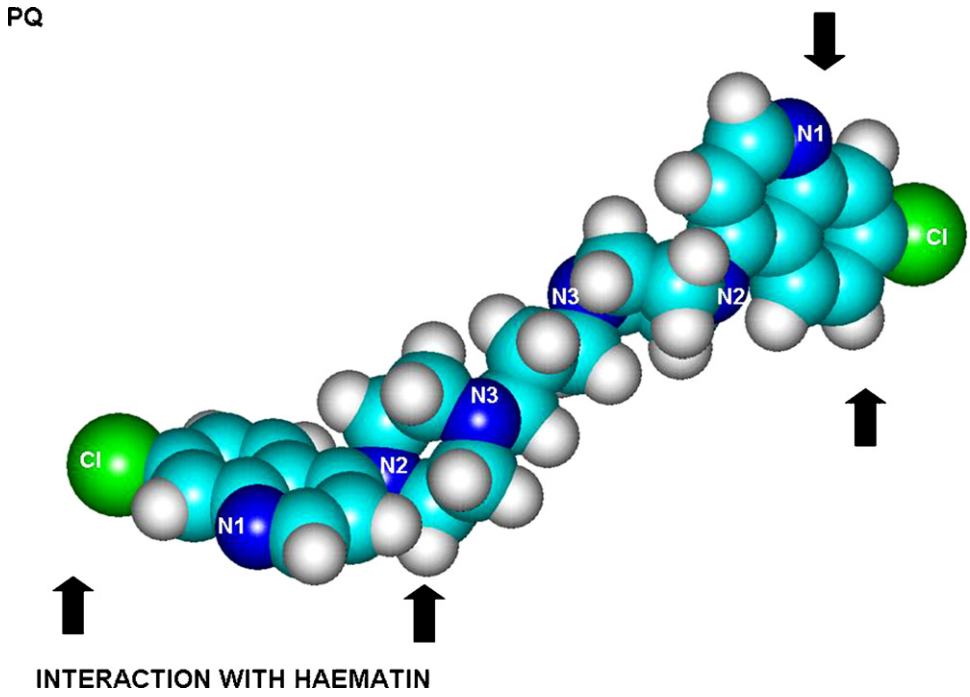

Fig. 4 – Calculated model of PQ base using AM1. The two aromatic heterocyclic areas likely to interact with haematin molecules are indicated. (Colours: C = light blue (unlabelled), H = grey (unlabelled), N = dark blue (labelled N1, N2 and N3), Cl = green (labelled Cl)). (For interpretation of the references to color in this figure legend, the reader is referred to the web version of the article.)

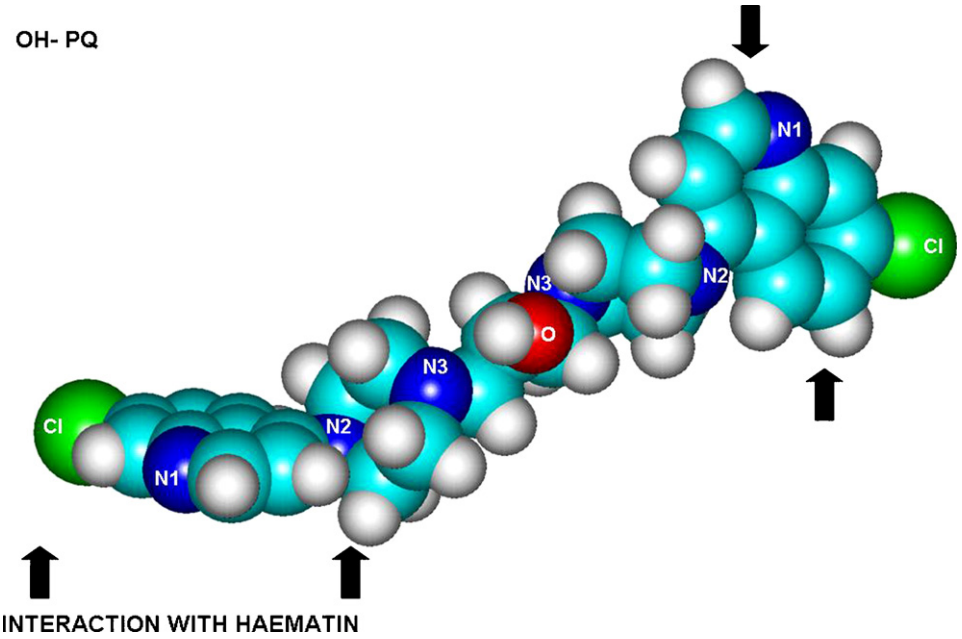

Fig. 5 – Calculated model of OH-PQ base using AM1. The two aromatic heterocyclic areas likely to interact with haematin molecules are indicated. (Colours: C = light blue (unlabelled), H = grey (unlabelled), N = dark blue (labelled N1, N2 and N3), Cl = green (labelled Cl) and O = red (labelled O).) (For interpretation of the references to color in this figure legend, the reader is referred to the web version of the article.)

4.2. *Drug activity and physicochemical features*

4.2.1. *A high VAR in addition to a suitable BHIA molar ratio is important for activity against CQ-S parasites*

Our observations on compounds **4** and **5** in comparison with CQ, PQ and OH-PQ support the detailed studies of Egan and colleagues on selected 4-amino-7-chloroquinolines [20,21], confirming that although binding to haematin and inhibition of its detoxication to β-haematin is an essential requirement for antimalarial activity of 4-amino-7-chloroquinolines against CQ-S parasites, there is a requirement for concentration of these agents to a suitable level within the acidic vacuole content before antiplasmodial activity can be manifested. While **4** and **5** are complementary parts of the *bis*-quinoline structure, showing the direct linking of the rigid piperazine ring through N-1′ to C-4 of the quinoline, different log $D_{(pH4.8)}$ values due to the presence of two rather than four protonatable N atoms per molecule mean that VAR values for **4** and **5** are low, at 1287 and 1966 compared with 104,378 and 19,874 for PQ and OH-PQ (Table 2). Table 3B shows a comparison of VAR and LAR in the drugs already studied with other 4-aminoquinolines, active or not in CQ-R, where the pK_a and log *P* values are available in the literature [e.g. 68] and can be used to calculate log *D*s. Desethylchloroquine (DECQ) and hydroxychloroquine (HCQ) have similar VAR values to CQ, and similar high activity in CQ-S. Their LAR values are also lower than CQ, and they are even less effective in CQ-R. In CQ-S, log IC_{50} is inversely proportional to log VAR. In a graphical analysis, although there was a linear relationship between the log of IC_{50} in CQ-S parasites (*y*) and log of VAR (*x*) for CQ, PQ, OH-PQ, **4** and **5** ($y = -1.0909x + 6.702$) which explained 94% of the variation ($P < 0.01$) there was a shortage of data for the middle of the line [not shown]. When values for the other 4-amino-7-chloroquinoline drugs [68] were included (Fig. 8), a linear relationship was retained, ($y = -1.0945x + 6.6921$) explaining 84% of variation ($P < 0.001$), although the centre of the curve was still short of data. The inverse relationship may be better described by a second order polynomial equation for a concave curve, which explains 94% of the variation (Fig. 8).

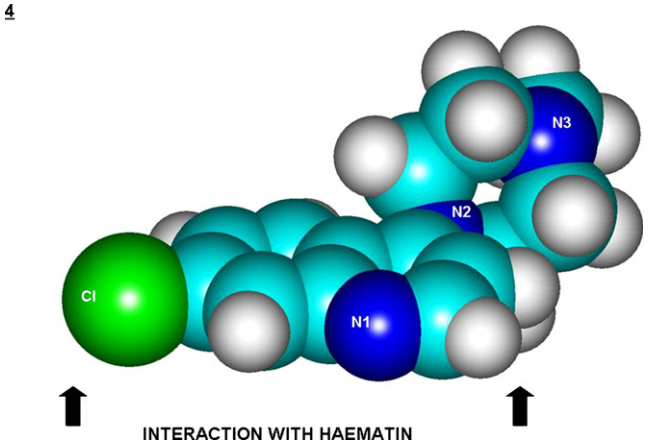

Fig. 6 – Calculated model of cpd. 4 Base using AM1. The aromatic heterocyclic area likely to interact with haematin is indicated. (Colours: C = light blue (unlabelled), H = grey (unlabelled), N = dark blue (labelled N1, N2 and N3), Cl = green (labelled Cl)). (For interpretation of the references to color in this figure legend, the reader is referred to the web version of the article.)

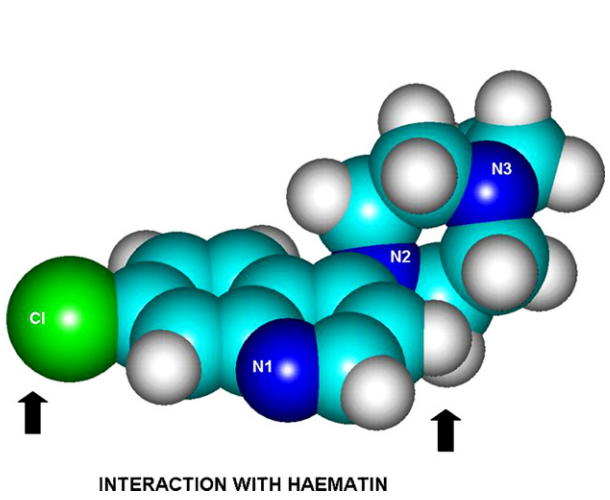

Fig. 7 – Calculated model of cpd. 5 Base using AM1. The aromatic heterocyclic area likely to interact with haematin is indicated. (Colours: C = light blue (unlabelled), H = grey (unlabelled), N = dark blue (labelled N1, N2 and N3), Cl = green (labelled Cl)). (For interpretation of the references to color in this figure legend, the reader is referred to the web version of the article.)

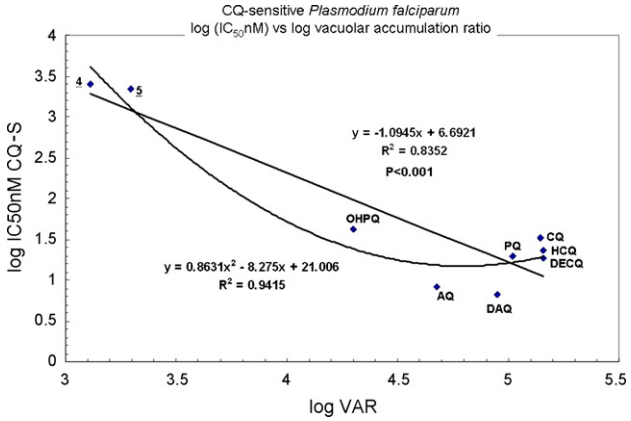

Fig. 8 – Chloroquine-sensitive *Plasmodium falciparum*, response to CQ and eight other 4-amino-7-chloroquinoline drugs. log IC_{50} (nM) (*y*) is plotted against log vacuolar accumulation ratio (VAR), (*x*). log IC_{50} is proportional to log VAR. This relationship is best described by a second order polynomial equation for a concave curve which explains 94% of the variation. Although a significant linear relationship is present, which explains 84% of variation ($P < 0.001$), there is a shortage of data in the central area of the line which casts doubt on the simplified linear interpretation. (DECQ: desethylchloroquine; DAQ: desethylamodiaquine; AQ: amodiaquine; HCQ: hydroxychloroquine.) The log *D* values which were used to calculate VAR were calculated from observed pK_a and log *P* values in this study and in Ref. [68].

While VAR is an important factor for activity in CQ-S, there appears no clear evidence that LAR plays any role, although LAR depends on VAR (see Section 2).

4.2.2. *4-Aminoquinolines with low resistance indices (RI) have higher LAR values, enabling the uncharged base to accumulate rapidly to high concentration in lipid*

Among 4-aminoquinolines readily inhibiting BIHA, those with a high VAR and a high LAR are likely to be effective in CQ-resistant parasites (Table 3B). DAQ and AQ have lower VAR values compared to CQ, and equal or better potency compared with CQ in CQ-S. Their LAR values are higher, and they are effective in CQ-R. PQ and OH-PQ have lower VAR values than CQ, and are similar in potency to CQ against CQ-S. However their LAR values are much higher than CQ, and they are effective in CQ-R. Compounds **4** and **5** have very low VAR values, and also are ~3 times less active in BHIA than CQ. They are very weakly active against *P. falciparum*. However, they have relatively high LAR values and **5** had a R.I. of only 2.03.

There is clear evidence of the importance of higher lipid distribution values (log *D*) in those 4-amino, 7-chloro quinolines active in CQ-R [29–32]. Furthermore, for a series of CQ and 7 other 4-amino-7-chloroquinoline drugs, the relationship between log R.I. and log LAR is a second order polynomial curve (Fig. 9), which, as the ordinate decreases regularly, can be separated into a straight line (Fig. 10) composed of six points explaining 85% of variation ($y = -0.4767x + 1.6841$) ($P < 0.01$), combined with a horizontal line parallel to the abscissa as the log R.I. approaches zero.

Success of 4-amino-7-chloroquinoline drugs with high LAR values could be explained by enhancement of β-haematin inhibition in vacuolar lipid where crystals of the detoxified product are produced [22], and/or may reflect their ability to

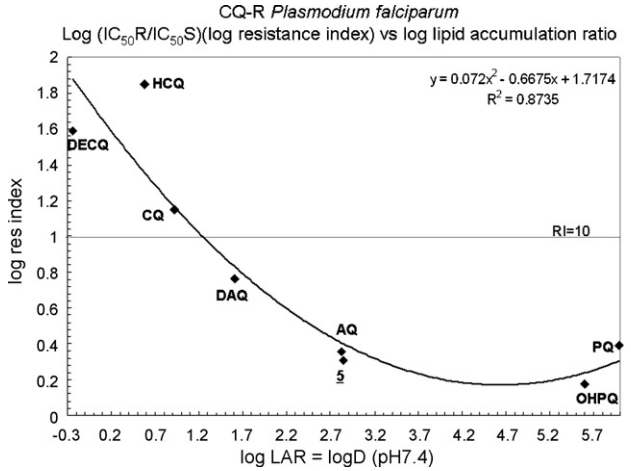

Fig. 9 – Log resistance index (IC_{50} nM of drug against CQ-R parasite/IC_{50} drug against CQ-S parasite) (*y*) for eight drugs is plotted against log LAR (*x*). This shows a second order polynomial relationship, which is probably composed of two straight lines, the first one is shown in Fig. 10, and the last one approximates to a horizontal line. LAR values were calculated from pK_a and log *P* values in this study and in Ref. [68]. (DECQ: desethylchloroquine; DAQ: desethylamodiaquine; AQ: amodiaquine; HCQ: hydroxychloroquine).

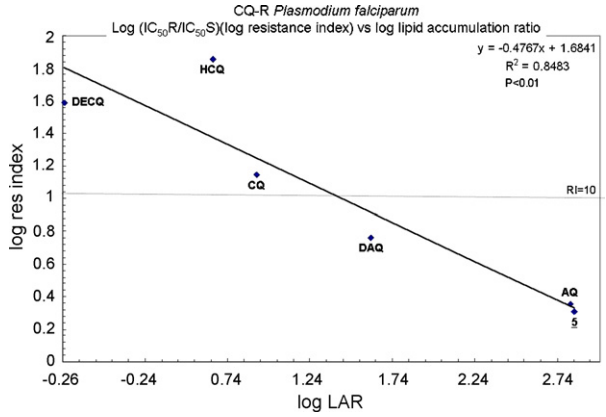

Fig. 10 – Log resistance index (IC_{50} drug against CQ-R parasite/IC_{50} drug against CQ-S parasite) (*y*) of a series of six 4-amino-7-chloroquinolines with different activities in CQ-resistance, omitting *bis* compounds PQ and OH-PQ, is plotted against log LAR (*x*). This shows the linear relationship ($P < 0.01$), describing the first part of the polynomial graph in Fig. 9. (DECQ: desethylchloroquine; DAQ: desethylamodiaquine; AQ: amodiaquine; HCQ: hydroxychloroquine; Compound 5).

block drug efflux by hydrophobic interaction with PfCRT [30,31]. It is intriguing to note that in CQ-S parasites, accumulation of charged drug in the vacuolar water (VAR) appears more important for activity, suggesting that interaction of these drugs with components of the modified hydrophobic channel in CQ-R PfCRT, which impedes efflux, may be the more important feature [30–32].

4.3. *Equilibrium modelling study: towards a mathematical description of the digestive vacuole in CQ-S and CQ-R parasites*

4.3.1. *CQ-sensitivity*

We have modelled at equilibrium the aqueous and membrane distribution of CQ and other drugs throughout the parasitized erythrocyte to determine their expected accumulation ratios between plasma (pH7.4) and vacuolar water (vacuolar accumulation ratio: VAR) and thence into vacuolar lipid (LAR) [53]. This confirms that while CQ2H+ concentration in vacuolar water (VAR) increases as vacuolar pH decreases, the concentration of uncharged CQ in vacuolar lipid membrane and lipid droplets remains constant because the proportion of drug from the vacuolar water partitioned into lipid (log *D*) decreases. Providing vacuolar pH is maintained at the steady low value (required for haemoglobin digestion) by inward proton pumping, unionized drug (CQ) passes through the vacuolar membrane and becomes concentrated as the ionized species (CQ2H+) in the vacuolar aqueous phase, to a steady high level (VAR) as a consequence of the pH gradient from the plasma. From the highly concentrated drug in the vacuolar aqueous phase, unionized CQ is distributed according to the log *D* at vacuolar pH into the vacuolar lipid and reaches the same concentration as in the erythrocyte membrane (LAR). The rate of distribution to lipid will depend on the concentration of CQ2H+ in the vacuolar water and the log *D* at vacuolar pH. This describes the situation in CQ-S parasites.

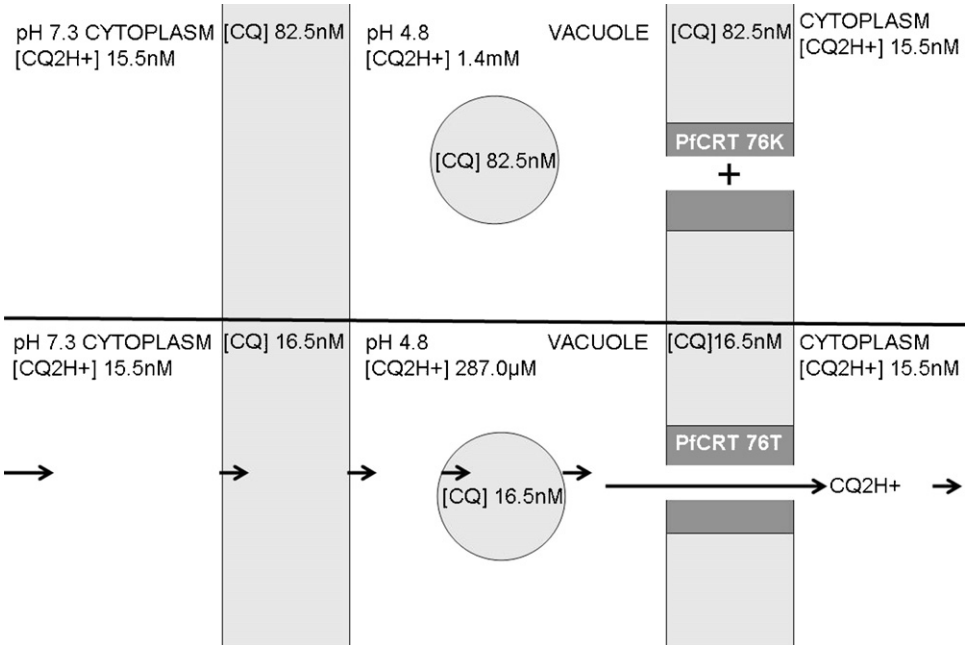

Fig. 11 – Top picture shows CQ-sensitive parasite at equilibrium. Lower picture shows snapshot of CQ-resistant parasite, with the lowest projected reduction (1/5) in overall uptake. CQ (concentration held at 10 nM) in medium (pH 7.4) enters the parasite cytoplasm from the RBC cytoplasm and becomes concentrated as CQ2H+ in the vacuolar water. In the lower picture, after the loss of + charge of K76, CQ2H+ is shown leaking through the CQ-resistant PfCRT) into the cytoplasm to be equilibrated through the RBC with the external medium.

4.3.2. *CQ-resistance*

In CQ-R parasites, CQ2H+ efflux through CQ-R PfCRT, will lower the concentration of CQ2H+ in vacuolar water without materially changing its pH. This will also reduce the transfer of CQ to vacuolar lipid (LAR). Assuming no material change in vacuolar pH, a drug efflux process through CQ-R PfCRT which effectively halves the CQ2H+ concentration in vacuolar water (VAR) to 0.5VAR ($VAR_{(CQR)}$) will, since $\log D_{(pH4.8)}$ remains the same, reduce LAR by the same factor (see Eq. (5)). Since estimates of at least 5 and at most 50 (depending on the experimental protocol) are reported for the [^{3}H]CQ equilibrium concentration ratio between CQ-S and CQ-R parasites (27,26), then $VAR_{(CQ\text{-}R)}$ of 28,696–2870, and $LAR_{(CQ\text{-}R)}$ of 1.65–0.165 can be expected in CQ-R parasites (for sketch, at CQ medium concentration 10 nM, see Fig. 11). However, the same calculation, applied to PQ will give an appreciably higher $LAR_{(CQ\text{-}R)}$ range of 194,698 to 19,470.

4.3.3. *Channel gating effects*

Bray et al. [27] have recently observed in de-energized conditions (in the absence of glucose or with 10 μM of the protonophore FCCP) increased steady-state uptake of [^{3}H]CQ by CQ-R *P. falciparum* similar to that observed in CQ-S under the same conditions, suggesting that the CQ-R PfCRT protein is a channel gated by membrane potential (proton gradient in this case). The CQ-R channel would be open and allow CQ2H+ efflux only in the presence of a trans-membrane pH difference, and be more or less closed when this is abolished or reduced. The effect of de-energization leading to a one unit rise in the normal vacuolar pH (according to the Nernst equation [76]) would be a reduction of 60 mV in vacuolar membrane potential which would partially gate the CQ-R passive efflux channel, increasing CQ-uptake and sensitivity.

Acknowledgements

The work was carried out while D.C. Warhurst and J.C. Craig were Emeritus Professors at: 1. The Department of Infectious and Tropical Diseases (Pathogen Molecular Biology Unit) of the London School of Hygiene and Tropical Medicine (LSHTM) (University of London) and 2. The Department of Pharmaceutical Chemistry of the University of California, San Francisco, respectively. Ipemida S. Adagu was a lecturer in Parasitology at LSHTM and Quinton L. Fivelman was supported there by a Commonwealth Research Fellowship. R. Kiplin Guy (associate professor) and Peter B. Madrid (postgraduate student, now a PhD) were working at the University of California, San Francisco.

Appendix A. Supplementary data

Supplementary data associated with this article can be found, in the online version, at doi:10.1016/j.bcp.2007.03.011.

REFERENCES

[1] Payne D. Spread of chloroquine resistance in *P. falciparum*. Parasitol Today 1987;3:241–6.
[2] Trape JF. The public health impact of chloroquine resistance in Africa. Am J Trop Med Hyg 2001;64:12–7.
[3] Raynes K. Bisquinoline antimalarials: their role in malaria chemotherapy. Int J Parasitol 1999;29:367–79.
[4] Schneider J, Bouvry M, Le Quellec J. *Plasmodium berghei* et chimiotherapie. Ann Soc Belge Med Trop 1965;45:435–49 (French).
[5] Benazet F. *Plasmodium berghei* et antimalariques a action de longue duree. Ann Soc Belge Med Trop 1965;45:459–66 (French).
[6] WHO. Chemotherapy of Malaria, Tech Rep Ser 375: Geneva; 1967.
[7] Benazet F. Activite d'un nouvel antimalarique, le 16126 RP, sur le paludisme experimental des animaux de laboratoire. Bull Soc Path Exot 1967;60:221–8 (French).
[8] Zhu DQ, Dai ZR, Li JC, Jiang ZK. Studies on piperaquine as long acting antimalarial drug. Acta Pharm Sinica 1982;17:894–8.
[9] Chen L, Qu FY, Zhou YC. Field observations on the antimalarial piperaquine. Chin Med J 1983;95:281–6.
[10] Vennerstrom JL, Ellis WY, Ager AL, Andersen SL, Gerena L, Milhous WK. Bisquinolines. 1. N, N-Bis (7-chloroquinolin-4-yl) alkanediamines with potential against chloroquine-resistant malaria. J Med Chem 1992;35:2129–34.
[11] Davis TM, Hung TY, Sim IK, Karunajeewa HA, Ilett KF. Piperaquine: a resurgent antimalarial drug. Drugs 2005;65:75–87.
[12] Ashley EA, McGready R, Hutagalung R, Phaiphun L, Slight T, Proux S, et al. A randomized, controlled study of a simple, once-daily regimen of dihydroartemisinin-piperaquine fo r the treatment of uncomplicated, multidrug-resistant falciparum malaria. Clin Infect Dis 2005;41:425–32.
[13] Chou AC, Chevli R, Fitch CD. Ferriprotoporphyrin IX fulfils the criteria for identification as the chloroquine receptor of malaria parasites. Biochemistry 1980;19:1543–9.
[14] Bray PG, Mungthin M, Ridley RG, Ward SA. Access to hematin: the basis of chloroquine resistance. Mol Pharmacol 1998;54:170–9.
[15] Warhurst DC, Hockley DJ. Mode of action of chloroquine on *Plasmodium berghei* and *P. cynomolgi*. Nature 1967;214:935–6.
[16] Homewood CA, Warhurst DC, Peters W, Baggaley VC. Lysosomes, pH and the antimalarial action of chloroquine. Nature 1972;235:50–2.
[17] Yayon A, Cabantchik ZI, Ginsburg H. Identification of the acidic compartment of *P. falciparum*-infected human erythrocytes as the target of the antimalarial drug chloroquine. EMBO J 1984;3:2695–700.
[18] Hayward R, Saliba KJ, Kirk K. The pH of the digestive vacuole of *Plasmodium falciparum* is not associated with chloroquine resistance. J Cell Sci 2006;119:1016–25.
[19] Pagola S, Stephens PW, Bohle DS, Kosar AD, Madsen SK. The structure of malaria pigment beta-haematin. Nature 2000;404:307–10.
[20] Egan TJ, Hunter R, Kaschula CH, Marques HM, Misplon A, Walden J. Structure–activity relationships in aminoquinolines: effect of amino and chloro groups on quinoline-haematin complex formation, inhibition of β-haematin formation and antiplasmodial activity. J Med Chem 2000;43:283–91.
[21] Kaschula CH, Egan TJ, Hunter R, Basilico N, Parapini S, Taramelli D, et al. Structure–activity relationships in 4-aminoquinoline antiplasmodials. The role of the group at the 7-position. J Med Chem 2002;45:3531–9.
[22] Pisciotta JM, Coppens I, Tripathi AK, Scholl PF, Shuman J, Bajad S, et al. The role of neutral lipid nanospheres in *Plasmodium falciparum* heme crystallization. Biochem J 2007;402:197–204.
[23] Egan TJ, Chen JY, de Villiers KA, Mabotha TE, Naidoo KJ, Ncokazi KK, et al. Haemozoin (beta-haematin)

biomineralization occurs by self-assembly near the lipid/water interface. FEBS Lett 2006;580:5105–10.
[24] Sullivan DJ, Gluzman IY, Russell DG, Goldberg DE. On the molecular mechanism of chloroquine's antimalarial action. Proc Natl Acad Sci USA 1996;93:11865–70.
[25] Fitch CD. *Plasmodium falciparum* in owl monkeys: drug resistance and chloroquine binding capacity. Science 1970;169:289–90.
[26] Krogstad DJ, Gluzman IY, Kyle DE, Oduola AM, Martin SK, Milhous WK, et al. Efflux of chloroquine from *Plasmodium falciparum*: mechanism of chloroquine resistance. Science 1987;238:1283–5.
[27] Bray PG, Mungthin M, Hastings IM, Biagini GA, Saidu DK, Lakshmanan V, et al. PfCRT and the trans-vacuolar proton electrochemical gradient: regulating the access of chloroquine to ferriprotoporphyrin IX. Mol Microbiol 2006;62:238–51.
[28] Fidock DA, Nomura T, Talley AK, Cooper RA, Dzekunov SM, Ferdig MT, et al. Mutations in the *P. falciparum* digestive vacuole transmembrane protein PfCRT and evidence for their role in chloroquine resistance. Mol Cell 2000;6:861–71.
[29] Bray PG, Hawley SR, Mungthin M, Ward SA. Physicochemical properties correlated with drug resistance and the reversal of drug resistance in *Plasmodium falciparum*. Mol Pharmacol 1996;50:1559–66.
[30] Warhurst DC, Craig JC, Adagu IS. Lysosomes and drug resistance in malaria. Lancet 2002;360(9345):1527–9.
[31] Warhurst DC. Polymorphism in the *Plasmodium falciparum* chloroquine-resistance transporter protein links verapamil enhancement of chloroquine sensitivity with the clinical efficacy of amodiaquine. Malar J 2003;2:31. Epub 2003 Sep 19.
[32] Johnson DJ, Fidock DA, Mungthin M, Lakshmanan V, Sidhu AB, Bray PG, et al. Evidence for a central role for PfCRT in conferring *Plasmodium falciparum* resistance to diverse antimalarial agents. Mol Cell 2004;15:867–77.
[33] Cooper RA, Hartwig CL, Ferdig MT. pfcrt is more than the *Plasmodium falciparum* chloroquine resistance gene: a functional and evolutionary perspective. Acta Trop 2005;94:170–80.
[34] Bennett TN, Kosar AD, Ursos LM, Dzekunov S, Singh Sidhu AB, Fidock DA, et al. Drug resistance-associated PfCRT mutations confer decreased *Plasmodium falciparum* digestive vacuolar pH. Mol Biochem Parasitol 2004;133:99–114.
[35] Krogstad DJ, Schlesinger PH. A perspective on antimalarial action: effect of weak bases on *P. falciparum*. Biochem Pharmacol 1986;35:547–52.
[36] Dewar MJS, Zoebisch EG, Healy EF, Stewart JJP. The development and use of quantum mechanical molecular models. 76. AM1: a new general purpose quantum mechanical molecular model. J Am Chem Soc 1985;107:3902–9.
[37] Dann O, Steuding W, Lisson KG, Seidel HR, Fink E, Nickel P. Antimalarial 6-aminoquinolines XV. 6- and 4-aminoquinolines with a tertiary basic alkylated amino group. Arzneim Forsch 1982;32:1219–23 (German).
[38] Kubinyi H. Lipophilicity and drug activity. In: Jucker E, editor. Progress in drug research, vol. 23. Basel: Birkhauser; 1979. p. 97–198.
[39] Rekker RF. The hydrophobic fragmental constant. Its derivation and application. A means of characterising membrane systems. In: Nauta WT, Rekker RF, editors. The hydrophobic fragmental constant, vol. 1. Amsterdam: Elsevier; 1977. p. 1–24.
[40] Hansch C, Leo AJ. Exploring QSAR fundamentals and applications in chemistry and biology, vol. 1. Washington, DC: American Chemical Society; 1995. 120.
[41] Scherrer RA, Howard SM. Use of distribution coefficients in quantitative structure–activity relationships. J Med Chem 1977;20:53–8.
[42] Leo AJ, Hansch C. Role of Hydrophobic effects in mechanistic QSAR. Perspect Drug Discov Des 1997;17:1–25.
[43] Van der Waterbeemd H, Testa B. The parametrization of lipophilicity and other structural properties in drug design. Adv Drug Res 1987;16:85.
[44] Avdeef A. pH-metric log *P*: refinement of partition coefficient and ionization constants of multiprotic substances. J Pharm Sci 1993;82:183–90.
[45] Avdeef A, Comer JEA, Thomson SJ. pH-Metric log *P*. III. Glass electrode calibration in methanol-water applied to pK_a determination of water-insoluble substances. Anal Chem 1993;65:42–9.
[46] Slater B, McCormack A, Avdeef A, Comer JEA. pH-Metric log *P* IV. Comparison of partition coefficients determined by HPLC and volumetric methods to literature values. J Pharm Sci 1994;83:1280–3.
[47] Additional material. ExCel spreadsheet for calculation of log *D* of a basic drug at a desired pH, from observed log *P* and pK_a values. "LOGDspreadsheet.xls" For downloading and to be run in Microsoft ExCel.
[48] Takacs-Novak K, Avdeef A. Interlaboratory study of log *P* determination by shake-flask and potentiometric methods. J Pharm Biomed Anal 1996;14:1405–13.
[49] Ryckebusch A, Deprez-Poulain R, Maes L, Debreu-Fontaine MA, Mouray E, Grellier P, et al. Synthesis and in vitro and in vivo antimalarial activity of N1-(7-chloro-4-quinolyl)-1, 4-bis(3-aminopropyl)piperazine derivatives. J Med Chem 2003;46:542–57.
[50] Walker O, Birkett DJ, Alvan G, Gustafsson LL, Sjoqvist F. Characterization of chloroquine plasma protein binding in man. Br J Clin Pharmacol 1983;15:375–7.
[51] Warhurst DC, Craig JC, Adagu IS, Meyer DE, Lee SY. The relationship of physico-chemical properties and structure to the differential antiplasmodial activity of the Cinchona alkaloids. Malar J 2003;2:26.
[52] Supanaranond W, Davis TM, Pukrittayakamee S, Silamut K, Karbwang J, Molunto P, et al. Disposition of oral quinine in acute falciparum malaria. Eur J Clin Pharmacol 1991;40:49–52.
[53] Additional material. Microsoft ExCel spreadsheet for calculation of distribution of a basic drug into membrane-bound compartments at desired pH, from log *D* values calculated from observed log *P* and pK_a values. "COMPARTMENTspreadsheet.xls" For downloading and to be run in Microsoft ExCel.
[54] Yayon A, Cabantchik ZI, Ginsburg H. Susceptibility of human malaria parasites to chloroquine is pH dependent. Proc Nat Acad Sci USA 1985;82:2784–8.
[55] Sillos EM, Shenep JL, Burghen GA, Pui C-H, Behm FG, Sandlund JT. Lactic acidosis: a metabolic complication of hematologic malignancies. Cancer 2001;92:2237–46.
[56] Agbenyega T, Planche T, Bedu-Addo G, Ansong D, Owusu-Ofori A, Bhattaram VA, et al. Population kinetics, efficacy, and safety of dichloroacetate for lactic acidosis due to severe malaria in children. J Clin Pharmacol 2003;43:386–96.
[57] Albert A. Selective toxicity, 5th ed., London: Chapman & Hall; 1973. p. 287.
[58] Egan TJ. Interactions of quinoline antimalarials with hematin in solution. J Inorg Biochem 2006;100:916–26.
[59] Parapini S, Basilico N, Pasini E, Egan TJ, Olliaro P, Taramelli D, et al. Standardization of the physicochemical parameters to assess in vitro the beta-haematin inhibitory activity of antimalarial drugs. Exp Parasitol 2000;96:249–56.
[60] Ncokazi KK, Egan TJ. A colorimetric high-throughput beta-haematin inhibition screening assay for use in the search

for antimalarial compounds. Anal Biochem 2005;338: 306–19.
[61] Thaithong S, Beale GH, Chutmongkonkul M. Susceptibility of *Plasmodium falciparum* to five drugs: an in vitro study of isolates mainly from Thailand. Trans Roy Soc Trop Med Hyg 1983;77:228–31.
[62] Rosario V. Cloning of naturally occurring mixed infections of malaria parasites. Science 1981;212:1037–8.
[63] Fivelman QL, Butcher GA, Adagu IS, Warhurst DC, Pasvol G. Malarone treatment failure and in vitro confirmation of resistance of *Plasmodium falciparum* isolate from Lagos. Niger Malar J 2002 Feb 8;1:1.
[64] Lambros C, Vanderberg JP. Synchronization of *Plasmodium falciparum* erythrocytic stages in culture. J Parasitol 1979;65:418–20.
[65] Angerman NS, Danyluk SS, Victor TA. A direct determination of the spatial geometry of molecules in solution. I. Conformation of chloroquine, an antimalarial. J Am Chem Soc 1972;94:7137–47.
[66] Preston HS, Stewart JM. Crystal structure of the antimalarial chloroquine diphosphate monohydrate. J Chem Soc Chem Commun 1970;1142–8.
[67] Perrin DD. Dissociation constants of organic bases in aqueous solutions (International Union of Pure and Applied Chemistry). London: Butterworth; 1965.
[68] Warhurst DC, Steele JCP, Adagu IS, Craig JC, Cullander C. Hydroxychloroquine is much less active than chloroquine against chloroquine-resistant *P. falciparum*. J Antimicrob Chemother 2003;52:188–93.
[69] Albert A, Goldacre R, Phillips JN. The strength of heterocyclic bases. J Chem Soc 1948;2240–9.
[70] Cruege F, Girault G, Coustal S, Lascombe J, Rumpf P. Contribution à l'etude des proprietes basiques de derives dimethylamines de la pyridine. Bull Soc Chim De France 1970;11:3889–94 (French).
[71] Albert A, Serjeant EP. The determination of ionization constants. London: Chapman & Hall; 1984. p. 157.
[72] Littel RJ, Bos M, Knoop GJ. Dissociation constants of some alkanolamines. J Chem Eng Data 1990;35:276–7.
[73] Leed A, DuBay K, Ursos LMB, Sears D, de Dios AC, Roepe PD. Solution structures of antimalarial drug-heme complexes. Biochemistry 2002;41:10245–5.
[74] De Dios AC, Casabianca LB, Kosar A, Roepe PD. Structure of the amodiaquine-FPIX μ oxo dimer solution complex at atomic resolution. Inorg Chem 2004;43:8078–84.
[75] De Dios AC, Tycko R, Ursos LMB, Roepe PD. NMR studies of chloroquine-ferriprotoporphyrin IX complex. J Phys Chem A 2003;107:5821–5.
[76] http://www.bmb.leeds.ac.uk/illingworth/oxphos/physchem.htm.